Earth Planets Space, **65**, 273–279, 2013

Clustering of far-infrared galaxies in the AKARI All-Sky Survey

A. Pollo[1,2,3], T. T. Takeuchi[4], T. L. Suzuki[4], and S. Oyabu[4]

[1]*National Centre for Nuclear Research, Hoża 69, 00-681 Warsaw, Poland*
[2]*Astronomical Observatory of the Jagiellonian University, Orla 171, 30-001 Cracow, Poland*
[3]*Center for Theoretical Physics of the Polish Academy of Sciences, Al. Lotnikow 32/46, 02-668 Warsaw, Poland*
[4]*Division of Particle and Astrophysical Science, Nagoya University, Furo-cho, Chikusa-ku, Nagoya 464-8602, Japan*

(Received December 15, 2011; Revised August 21, 2012; Accepted August 22, 2012; Online published March 12, 2013)

We present the first measurement of the angular two-point correlation function for AKARI 90-μm point sources, detected outside of the Milky Way plane and other regions characterized by high Galactic extinction, and categorized as extragalactic sources according to our far-infrared-color based criterion (Pollo *et al.*, 2010). This is the first measurement of the large-scale angular clustering of galaxies selected in the far-infrared after IRAS measurements. Although a full description of the clustering properties of these galaxies will be obtained by more detailed studies, using either a spatial correlation function, or better information about properties and, at least, photometric redshifts of these galaxies, the angular correlation function remains the first diagnostic tool to establish the clustering properties of the catalog and the observed galaxy population. We find a non-zero clustering signal in both hemispheres extending up to ∼40 degrees, without any significant fluctuations at larger scales. The observed correlation function is well fitted by a power-law function. The notable differences between the northern and southern hemispheres are found, which can probably be attributed to the photometry problems, and might point to the necessity of performing a better calibration in the data from the southern hemisphere.
Key words: Galaxies: clustering, large scale structure, dust, infrared, cosmology.

1. Introduction

According to the now widely-accepted paradigm of the gravitational instability theory, galaxies formed and evolved inside dark matter halos. These haloes grew and merged under the effect of gravity, starting from the primordial, almost homogeneous, distribution, which is imprinted in the cosmic microwave background (see, e.g. White and Rees, 1978). Analysis of the galaxy clustering is then believed to be the key to understanding the evolution of the underlying dark matter field, and hence the Universe itself. It is therefore an important issue to understand the bias between the distribution of galaxies and the underlying dark matter density field, and how it depends on galaxy properties.

The Infrared Astronomical Satellite (IRAS: Neugebauer *et al.*, 1984) has achieved a great amount of statistics. Especially in cosmology, the IRAS Point Source Catalog (PSC) has provided a great homogeneous dataset of galaxies which has driven statistical studies drastically. A vast number of studies have been carried out based on IRAS galaxies. Early studies were based on the angular correlation (Meiksin and Davis, 1986; Rowan-Robinson and Needham, 1986; Babul and Postman, 1990; Lahav *et al.*, 1990; Liu *et al.*, 1994). Later, thanks to various IRAS redshift surveys (e.g., Rowan-Robinson *et al.*, 1991; Strauss *et al.*, 1992; Fisher *et al.*, 1995; Saunders *et al.*, 2000), tremendous progress has been made in spatial distribution or correlation function analysis (e.g., Efstathiou *et al.*, 1990; Saunders *et al.*, 1992; Hamilton, 1993; Fisher *et al.*, 1994; Peacock, 1997). In these studies, IR galaxies have been used as a tracer of total baryonic mass contained in galaxies, explicitly or implicitly.

However, this might not be regarded as an appropriate assumption anymore, since it was found that the amount of dust in galaxies not in all cases is strongly correlated to the stellar mass (e.g., Iyengar *et al.*, 1985; Tomita *et al.*, 1996). Indeed, a significant relative bias of IRAS galaxies to optical ones was found (e.g., Babul and Postman, 1990; Lahav *et al.*, 1990; Peacock and Dodds, 1994). Nowadays, the IR emission from galaxies is known to be a good tracer of star formation activity, especially for actively star-forming galaxies, through the heating of dust grains by OB stars (e.g., Buat *et al.*, 2007; Takeuchi *et al.*, 2010; Murphy *et al.*, 2011). Therefore, in a modern context, the large-scale structure of dusty galaxies is regarded as the star-formation density field in galaxies, which may be important to connect the dark matter field and star formation activity (e.g., Małek *et al.*, 2010; Amblard *et al.*, 2011).

This view has been supported by a vast number of analyses of the clustering of infrared galaxies, at scales up to a few degrees, in various surveys. After IRAS, IR correlation functions have been mainly estimated based on deep surveys. Gonzalez-Solares *et al.* (2004) estimated the angular correlation function of ISO 15-μm galaxies in the European Large-Area Infrared Space Observatory (ELAIS) S1 survey. From ISO deep surveys, Matsuhara *et al.* (2000) and Lagache and Puget (2000) performed a power spectrum analysis of the diffuse far-infrared (FIR) background

doi:10.5047/eps.2012.08.009

and discovered fluctuations due to the large-scale clustering of dusty galaxies. Subsequently, angular clustering analyses of Spitzer surveys have been published (e.g., Oliver *et al.*, 2004; de la Torre *et al.*, 2007; Gilli *et al.*, 2007; Magliocchetti *et al.*, 2008). These works are mainly based on mid-infrared (MIR) data, but thanks to Herschel, recently, results from longer wavelengths have been gradually reported (e.g., Cooray *et al.*, 2010; Maddox *et al.*, 2010; Amblard *et al.*, 2011; Magliocchetti *et al.*, 2011; Planck Collaboration *et al.*, 2011).

After many years since IRAS, the advent of AKARI (ASTRO-F) opened new possibilities to explore the whole sky in the far infrared, as a survey-oriented space telescope at MIR and FIR (Murakami *et al.*, 2007). The primary purpose of the AKARI mission is to provide second-generation infrared (IR) catalogs to obtain a better spatial resolution and a wider spectral coverage than the IRAS catalog. All-sky surveys and some pointed deep observations were made by AKARI. In this work, we present the first measurement of the angular correlation function for FIR-selected extragalactic sources from the AKARI All-Sky Survey. Some related works on the AKARI Deep Field-South (ADF-S) have been published: Małek *et al.* (2010) have performed an attempt to identify the FIR-bright extragalactic sources and used their correlation function to estimate the limitations of completeness of the sample due to source confusion, while Matsuura *et al.* (2011) measured the power spectrum of the cosmic infrared background (CIB) in the ADF-S, providing a new upper limit for the clustering properties of distant infrared galaxies and any diffuse emission from the early universe which might have contributed to the CIB. However, in this work, we have made an analysis on much wider area data to see the large-angle correlation.

This article is organized as follows: in Section 2, we present the selection of data used for this analysis. In Section 3, we present and discuss the properties of the angular correlation function of selected AKARI sources. We present a Summary and Conclusions in Section 4.

2. Data

2.1 AKARI

AKARI is a Japanese astronomical satellite the purpose of which is to perform various large-area surveys at the IR wavelengths, from near- to far-infrared (NIR to FIR), with a wavelength coverage of 2–160 μm, as well as pointed observations.[1] AKARI is equipped with a cryogenically cooled telescope of 68.5 cm aperture diameter and two scientific instruments, the Far-Infrared Surveyor (FIS; Kawada *et al.*, 2007) and the Infrared Camera (IRC; Onaka *et al.*, 2007).

2.2 AKARI all-sky surveys

Among the most significant astronomical observations performed by AKARI, an all-sky survey with FIS and IRC has been carried out: referred to as the AKARI All-Sky Survey. It is the second ever performed all sky survey at FIR, after IRAS. The FIS scanned 96% of the entire sky more than twice in the 16 months of the cryogenic mission phase. In March 2010, the AKARI/FIS Bright Source Catalogue v.1.0 was released to the scientific community. It contains in total 427071 point sources measured at 65, 90, 140, 160 μm. Hereafter, we use the notation S_{65}, S_{90}, S_{140} and S_{160} for flux densities in these bands.

The position accuracy of the FIS sources is $8''$, since the source extraction is made with grids of this size. The effective size of the point spread function of AKARI FIS in FWHM is estimated to be $37 \pm 1''$, 39 ± 1, $58 \pm 3''$, and $61 \pm 4''$ at 65 μm, 90 μm, 140 μm, and 160 μm, respectively (Kawada *et al.*, 2007). Errors are not estimated for each individual source, but instead they are, in total, estimated to be 35%, 30%, 60%, and 60% at 65 μm, 90 μm, 140 μm, and 160 μm, respectively (Yamamura *et al.*, 2010).

The AKARI All-Sky Survey, and, in particular, the sample used in this paper for the measurement of the angular correlation function of extragalactic sources, differs in many details from its precursor: the IRAS sample. First of all, IRAS samples used for similar studies were based on 60-μm measurements, while the AKARI survey is based on the 90-μm band. The depth of the IRAS survey was estimated to be $S_{60} \geq 0.6$ Jy (Rowan-Robinson and Needham, 1986), while the formal depth of the AKARI FIS All-Sky Survey is $S_{90} \geq 0.2$ Jy. The angular resolution of AKARI is also better: less than $1'$ at the longest wavelengths, while the resolution of IRAS was $\sim 2'$.

Consequently, the properties of objects observed by AKARI in the All-Sky Survey are not exactly the same as those of the IRAS sources. Since FIS has a greater sensitivity at longer wavelengths than IRAS, we can expect a different composition of sources: we should see objects with cool dust which were difficult to detect by IRAS bands. Consequently, the clustering properties of galaxies selected from the AKARI FIS catalogs can also be different from the corresponding IRAS galaxies.

2.3 Selection of extragalactic sources

As mentioned before, the complete FIS All-Sky Survey contains 427071 point sources. Since the primary detection was performed at 90 μm, all sources have a flux measurement at least at this band.

In the subsequent analysis, we restrict ourselves to the area of low contamination from the Galactic FIR emission ($I_{100} \leq 5$ MJy sr^{-1}) measured from the Schlegel maps (Schlegel *et al.*, 1998), in order to avoid contamination by sources from the Galactic plane and Galactic cirrus emission. This procedure excludes also areas of both Magellanic Clouds. This is the most severe restriction, since the majority of the All-Sky Survey sources lay in these heavily-extincted areas: The applied procedure leaves us with 30323 sources.

In Pollo *et al.* (2010), we have presented a method to classify the AKARI sources in the color-color diagrams only from FIS bands. In order to be able apply this method to select candidates for extragalactic sources in the following analysis, we further restrict ourselves only to sources which were detected at least at 65 μm, 90 μm and 140 μm, with an additional condition of the high-quality flag of S_{90} ($f_{90} = 3$, meaning sure detection and secure flux measurement). These conditions were chosen to assure a reasonably high quality of the data, but keeping the numbers of sources

[1] Detailed information on the AKARI project, instruments, data and important results can be found via URL: http://www.ir.isas.ac.jp/ASTRO-F/index-e.html.

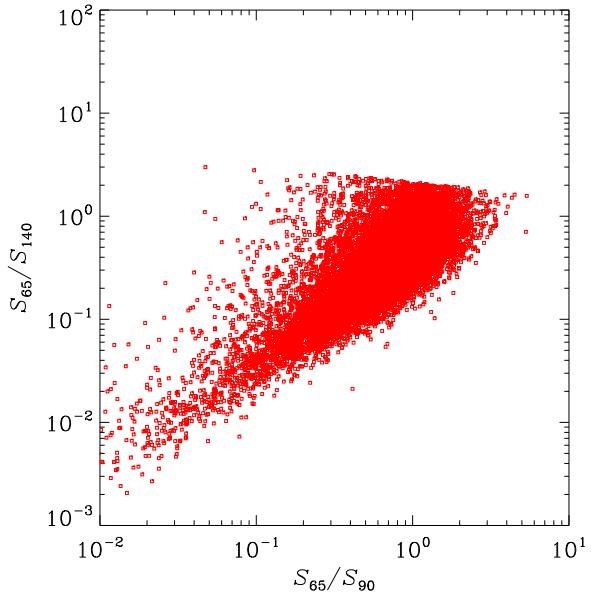

Fig. 1. Color selection of AKARI FIS 90-μm sources. Galaxy candidates are presented by dots.

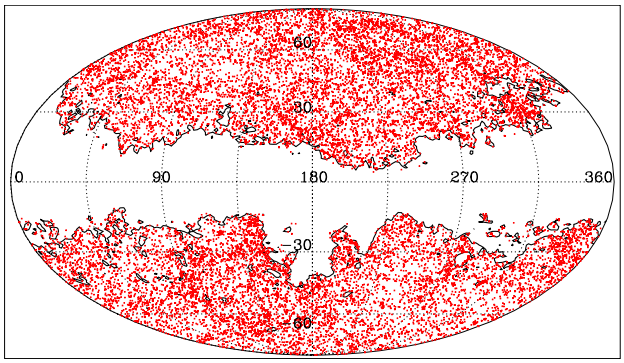

Fig. 2. Sky distribution of AKARI FIS galaxies selected by colors, plotted in the Galactic coordinates. Only galaxies located on the sky region with $I_{100} < 5$ MJy sr^{-1} are used in this analysis.

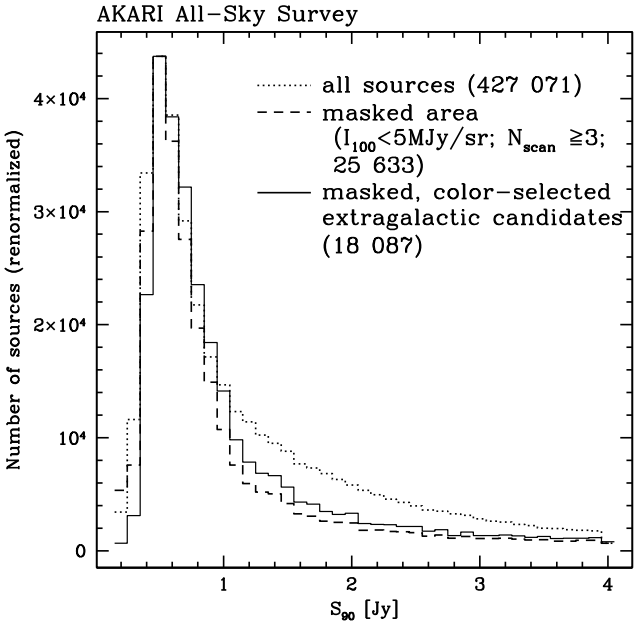

Fig. 3. Renormalized histograms of S_{90} fluxes of AKARI FIS sources. The dotted line corresponds to the sources from the complete sample. Sources from the masked areas, i.e. areas with Galactic cirrus emission lower than 5 MJy sr^{-1} and scanned by AKARI at least three times, are denoted by solid line. Sources from the masked area, selected as galaxy candidates by our far infrared color-based criterion, are shown by the dashed line.

used for the subsequent analysis possibly high. From our sample, 21008 sources fulfill these requirements.

Then, we applied our color-based method to select candidates for the extragalactic sources in the low-extinction area. As a result, 19806 (i.e. ∼94% of the sample) objects were classified as extragalactic sources, while 1202 sources (i.e. ∼6% of the sample) were classified as stars. According to Pollo *et al.* (2010), the expected contamination of the extragalactic population by stars is ∼4%, while the risk of a galaxy being misidentified as a star is ∼17%. However, these errors were estimated for the sample constructed without any restriction for the quality of the flux measurements. Further, yet unpublished tests (Rybka *et al.*, 2012, 2013), have shown that using only high-quality flags we improve these errors significantly; and while some of the Galactic sources remain classified as extragalactic—this applies, for example, to planetary nebulae due to their intrinsic properties—the risk of misclassification of a galaxy as a star drops down to ∼2–3%. Then, given our selection criteria, we expect the contamination of both Galactic and extragalactic groups classified by our algorithm, to be of the order of 2–4%. The result of this selection of extragalactic sources on the S_{65}/S_{90} vs S_{65}/S_{140} color-color plane is presented in Fig. 1.

In order to assure a good quality of AKARI photometric measurements, we additionally masked the data, restricting ourselves only to the parts of the sky which were scanned by AKARI at least three times. This masking procedure reduced the final sample by further ∼9%, leaving us with 18087 candidates for extragalactic sources: 9700 from the northern hemisphere, and 8387 from the southern hemisphere.

The sky distribution of all these 18087 sources, left after masking and selection procedures, is presented, in the Galactic coordinates, in Fig. 2. This sample is then used for the analysis presented in the next sections.

The results of our selection procedure on S_{90} luminosities of the sample can be seen in Fig. 3 which presents the renormalized histograms of S_{90} for the complete sample, masked sample and masked sample of color-selected galaxies. We can see that the masking procedure significantly reduces the bright tail of the distribution by the removal of the brightest Milky Way sources. The color selection seem to partially reverse this effect, which is a result of the fact that only sources with full color information, systematically brighter, were used for this procedure. A few remaining sources with the value of S_{90} lower than 0.2, which is below the 3 σ detection limit of AKARI, were also excluded from the further analysis.

The procedure aiming at the construction of the clean and secure catalog of extragalactic sources, described above, may also lead to differences in their measured clustering

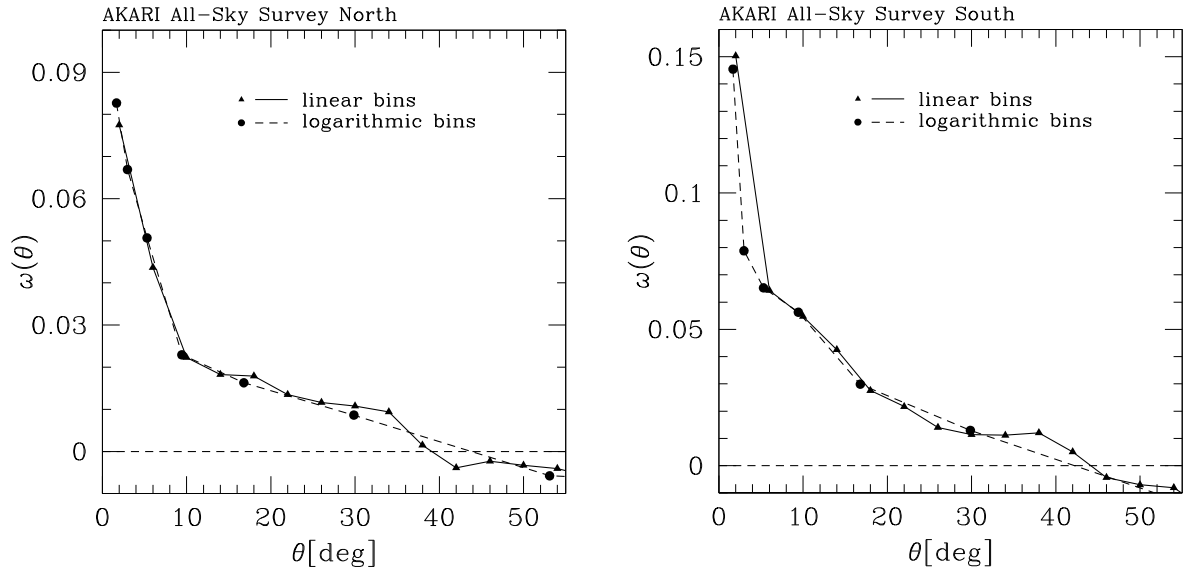

Fig. 4. Angular correlation function, in linear and logarithmic bins, in the northern (left panel) and southern (right panel) hemisphere of the AKARI All-Sky Survey. In both panels linear bins are marked by full triangles, connected by a solid line, while logarithmic bins are shown as full circles connected by a dashed line. Note the difference in scale of the panels.

properties, when compared to IRAS. In the first IRAS analysis, the masking conditions were based primarily on selecting the high Galactic latitude sources, e.g. $|b| > 30^o$ by Rowan-Robinson and Needham (1986), or $|b| > 10^o$ by Meiksin and Davis (1986), and excluding areas heavily affected by Galactic cirrus. The selection of extragalactic sources was usually based on the color-related criterion; however, in contrast to our case, a difference between the FIR (at 60 μm) and MIR flux—at 25 μm in Rowan-Robinson and Needham (1986), or 12 μm in Meiksin and Davis (1986)—was taken into account. Since our method is only FIR-based, it increases the possibility that sources dominated by the emission from the cool dust, but without counterparts at shorter wavelengths, would be taken into account. These methods used in IRAS analysis resulted in the selection of 5000 to 6000 "secure" galaxies brighter than $S_{60} = 0.6$ Jy in all the sky. With our method, with a depth comparable to IRAS but at a longer wavelength, i.e. with $S_{90} > 0.6$ Jy, we get 8592 sources.

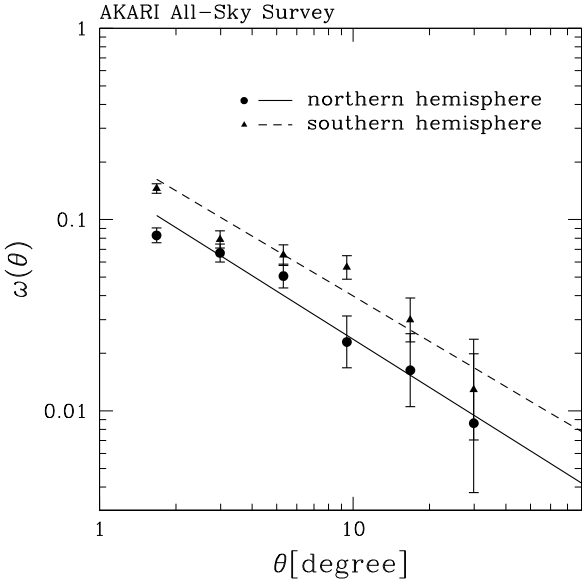

Fig. 5. Power-law fit to the angular correlation function of extragalactic sources, measured in the northern (full circles, solid line) and southern (full triangles, dashed line) hemisphere of the AKARI All-Sky Survey. Points correspond to the measurements in the logarithmic bins, while lines show the best power-law fit.

3. Clustering of AKARI All-Sky Survey Galaxies

3.1 Method

The two-point angular correlation function, $\omega(\theta)$, is defined as the excess probability above random that a pair of galaxies is observed at a given angular separation θ (Peebles, 1980). It is the simplest statistical measurement of clustering, as a function of angular scale, and it corresponds to the second moment of the distribution. Various recipes, aiming at minimizing different sorts of observational biases, have been proposed to estimate two-point correlation functions from galaxy surveys. In this work, we adopt the angular version of the Landy-Szalay estimator (Landy and Szalay, 1993), which expresses $\omega(\theta)$ as

$$\omega(\theta) = \frac{N_R(N_R-1)}{N_G(N_G-1)}\frac{GG(\theta)}{RR(\theta)} - \frac{N_R-1}{N_G}\frac{GR(\theta)}{RR(\theta)} + 1 \quad . \quad (1)$$

In this expression, N_G and N_R are the total number (equivalently, the mean density may be used) of objects, respectively, in the galaxy sample and in a catalog of random points distributed within the same survey volume, and with the same photometric mask applied as the one used for the real data. $GG(\theta)$ is the number of independent galaxy-galaxy pairs with a separation between θ and $\theta + d\theta$; $RR(\theta)$ is the number of independent random-random pairs within the same interval of separations, and $GR(\theta)$ represents the number of galaxy-random pairs.

Different ways of estimating errors on two-point cor-

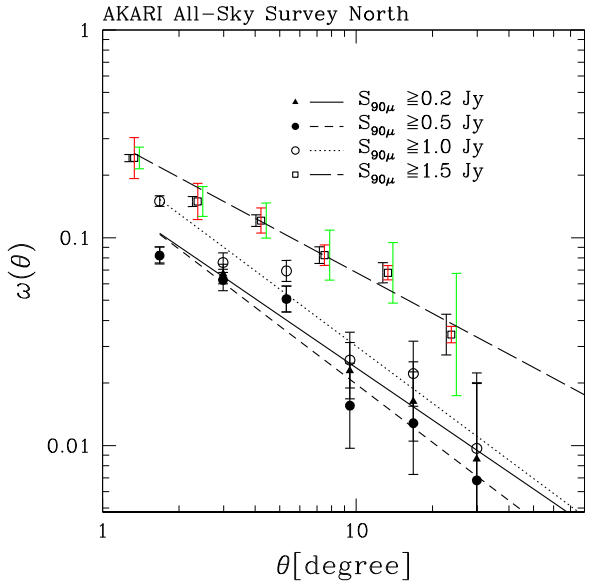

Fig. 6. Angular correlation function in the AKARI All-Sky Survey North—comparison of subsamples with different limits of flux density S_{90}. Points correspond to the measurements in the logarithmic bins and lines show the best power-law fit. Full triangles and the solid line correspond to the whole sample, i.e. $S_{90} > 0.2$ Jy. Full circles and the short-dashed line correspond to the sample with a limit $S_{90} > 0.5$ Jy. Open circles and the dotted line correspond to the sample limited by $S_{90} > 1$ Jy. The brightest sample $S_{90} > 1.5$ Jy is shown by open squares and the long-dashed line. Error bars are ensemble errors, in all cases, bar the one for the brightest sample ($S_{90} > 1.5$ Jy), where three possible error bars: Poissonian (central error bar), analytical estimations for ensemble (left error bar) and bootstrap (right error bar) are shown.

relation functions have been described in the literature (Hamilton, 1993; Fisher *et al.*, 1994; Norberg *et al.*, 2009). Since our aim, in this case, is the first diagnosis of the galaxy clustering in the AKARI data, we do not apply any refined error estimation method. As widely discussed in the literature (see, e.g., Fisher *et al.*, 1994), Poissonian errors usually indicate only the lower limit on the actual errors, since they simply reflect the information related to the statistical properties of the sample. In this paper, for simplicity, we apply the analytic estimation of the expected errors based on the approach introduced by Mo *et al.* (1992).

For the clarity of the presentation, in Fig. 4, which presents the large-scale behaviour of the angular correlation function in the linear scale, we do not include error bars. In Figs. 5 and 6, we present the expected ensemble errors on the values of the correlation function, based on the Mo *et al.* (1992) method, with the due corrections related to the fact that we use a different estimator for the correlation function (Landy and Szalay estimator instead of the so-called natural estimator). In Fig. 6, for the brightest subsample ($S_{90} \geq 1.5$ Jy) only, we present, in different colors, three possible error bars: Poissonian errors, ensemble errors, and bootstrap errors. Since Poissonian errors underestimate the actual errors, and bootstrap errors are known to overestimate them, the ensemble errors in our case may give a fair estimation of the actual values.

In practice, both the spatial and angular correlation functions are usually well fitted by a power-law model:

$$\omega(\theta) = A_w \theta^{1-\gamma}, \qquad (2)$$

with $1 - \gamma$ being the slope of the correlation function (γ itself is then the slope of a corresponding spatial correlation function) and A_w is the normalization of the correlation function.

3.2 Clustering of sources in southern and northern hemispheres

The angular correlation function in the linear scale is shown, separately for the northern and southern Galactic hemispheres, in the left and right panels, correspondingly, of Fig. 4. In both hemispheres we measure a positive signal up to $\theta \sim 40$ degrees. For separations larger than ∼40 degrees, the signal remains negative without any significant fluctuations. This roughly agrees with the first clustering measurement for the IRAS sources (Rowan-Robinson and Needham, 1986). In contrast to what was seen in the first IRAS data, we do not observe any strong difference in the shape of the correlation function between the northern and southern sky; in particular, between 10 and 40 degrees. However, there are notable differences: the most important is that sources in the southern sky seem to be, at all scales, more strongly clustered than those observed in the northern sky. This discrepancy between both hemispheres remains visible, and similar in amplitude, also if more severe restrictions on the Galactic extinction are applied ($I_{100} \leq 10$ MJy sr^{-1}, $I_{100} \leq 15$ MJy sr^{-1}).

Since this feature does not correspond to any feature ever measured in other wavelengths, the most probable explanation of this fact would be imperfect calibration of photometry of the data from the southern hemisphere. Another possibility may be related to still-remaining effects of Galactic extinction at high Galactic latitudes, due to, for example, imperfectly-treated cirrus, or contamination from Galactic sources. Finally, the least plausible, in our opinion, but still open to debate, is the possibility that the observed effect is due to cosmic variance, which would be in this case changing with galaxy properties. This issue will be better analyzed in future papers.

A similar problem was also realized in the case of the first IRAS data (e.g., Rowan-Robinson and Needham, 1986). Our results indicate, then, that the All-Sky Survey data should still be approached with some caution until the reasons for this discrepancy are clarified.

The difference between both hemispheres becomes even clearer when we a power-law fit to the angular correlation function is made, as shown in Fig. 5. Both correlation functions can be fitted by the power-law function reasonably well on the scale 1–40 degrees, but some scale-dependent deviations are clearly visible in the function measured in the southern hemisphere. Both functions have a very similar slope $\gamma = 1.8 \pm 0.1$, higher than previously measured for these scales for FIR galaxies. From this plot, it is also well visible that southern galaxies seem to be much more strongly clustered than northern ones, with the clustering length $A_w = 0.24 \pm 0.01$ degrees, while in the northern hemisphere we measure $A_w = 0.16^{+0.02}_{-0.01}$.

3.3 Flux density dependence of clustering in the AKARI All-Sky Survey North

The dependence of the clustering properties of AKARI FIS galaxies on their flux density in 90 μm is presented in Fig. 6 and Table 1. A general trend is the agreement with the

Table 1. Clustering properties of four subsamples with a different flux density S_{90} in the AKARI All-Sky Survey North.

Limiting S_{90} [Jy]	Number of galaxies	A_w [deg]	γ
0.2	8472	$0.16^{+0.02}_{-0.01}$	1.8 ± 0.1
0.5	5493	0.16 ± 0.02	1.9 ± 0.1
1.0	2233	$0.24^{+0.05}_{-0.04}$	1.9 ± 0.2
1.5	1282	$0.30^{+0.07}_{-0.05}$	$1.7^{+0.1}_{-0.1}$

behavior expected from the hierarchical model of structure formation, and with other similar measurements: brighter galaxies are clustered were strongly than fainter ones, and the clustering length increases with the limiting flux density. The reversal of this trend can be observed in the case of the two faintest samples: galaxies with $S_{90} > 0.5$ Jy seem to be less clustered than the complete sample limited by $S_{90} > 0.2$ Jy. This latter result might indicate that the photometric measurements are systematically biased for some of the faintest sources. The clustering of the brightest subsample is the strongest, and the best-fitted slope is less steep than in the case of fainter sources, which is more similar to other far-infrared surveys.

Comparison to similar IRAS results (see e.g. Meiksin and Davis, 1986 table II), not precise because of different ranges and a different choice of the sample, reveals that sources of a similar FIR brightness, in both cases, have close clustering amplitudes. This measurement would imply that, after all, with the selection applied, we observed with AKARI at 90 μm a similar field of nearby star-forming galaxies as IRAS did at 60 μm. More detailed differences between these populations might be revealed by more precise studies. At the same time, the slope γ of the correlation function of AKARI galaxies is significantly higher, close to γ measured for optically-detected galaxies. A possible reason is a better angular resolution of AKARI, and a resulting better recovery of galaxy pairs at smaller angular scales.

4. Summary and Conclusions

We present the first measurement large-scale clustering of far-infrared galaxies in the AKARI FIS All-Sky Survey. We have measured the angular two-point correlation function for the 90-μm-selected sample of galaxies in the northern and southern hemisphere. Our conclusions are as follows:

1) We find a positive signal up to $\sim$40 degrees, in all scales between 1 and 40 degrees, reasonably well fitted by a single power-law function with $\gamma \sim 1.8 \pm 0.1$, and the amplitude $A_w = 0.16^{+0.02}_{-0.01}$ for the northern, and 0.24 ± 0.01 for the southern, hemisphere.
2) We suggest that this north-south difference might be a result of calibration problems in the data due to the southern hemisphere, or still-remaining effects of Galactic cirrus or contamination from Galactic sources. The cosmic variance, even if not very plausible, as the cause of the total effect should also be taken into account.
3) We observe an increase of clustering length with increasing flux density limit of the sources, in accordance with expectations for a sample of relatively-nearby galaxies.

This measurement of clustering for dusty galaxies is the first in the series and it shows the potential of the AKARI data for this type of study. Future measurements, performed after a better understanding of the data, and including the identification of sources and their redshift information, will make it possible to relate the density field of galaxies with hidden strong star-forming activity to the general population of galaxies, i.e., the relative bias of dusty star-forming galaxies.

Acknowledgments. We would like to express our deep gratitude to the referees: Prof. Hideo Matsuhara and another anonymous referee, for their thorough, constructive and helpful comments. This work is based on observations with AKARI, a JAXA project with the participation of ESA. AP has been supported by the research grant of the Polish National Science Centre N N203 51 29 38. This research was partially supported by the project POLISH-SWISS ASTRO PROJECT co-financed by a grant from Switzerland through the Swiss Contribution to the enlarged European Union. TTT has been supported by the Grant-in-Aid for the Scientific Research Fund (20740105, 23340046) commissioned by the MEXT. TTT, TLS, and SO have also been partially supported from the Grand-in-Aid for the Global COE Program "Quest for Fundamental Principles in the Universe: from Particles to the Solar System and the Cosmos" from the Ministry of Education, Culture, Sports, Science and Technology (MEXT) of Japan.

References

Amblard, A. *et al.*, Submillimetre galaxies reside in dark matter haloes with masses greater than 3×10^{11} solar masses, *Nature*, **470**, 510–512, 2011.

Babul, A. and M. Postman, IRAS galaxies and the large-scale structure in the CfA slice, *Astrophys. J.*, **359**, 280–290, 1990.

Buat, V. *et al.*, The local universe as seen in the far-infrared and far-ultraviolet: A global point of view of the local recent star formation, *Astrophys. J. Suppl. Ser.*, **173**, 404–414, 2007.

Cooray, A. *et al.*, HerMES: Halo occupation number and bias properties of dusty galaxies from angular clustering measurements, *Astron. Astrophys.*, **518**, L22, 2010.

de la Torre *et al.*, VVDS-SWIRE. Clustering evolution from a spectroscopic sample of galaxies with redshift $0.2 < z < 2.1$ selected from Spitzer IRAC 3.6 μm and 4.5 μm photometry, *Astron. Astrophys.*, **475**, 443–451, 2007.

Efstathiou, G., N. Kaiser, W. Saunders, A. Lawrence, M. Rowan-Robinson, R. S. Ellis, and C. S. Frenk, Large-scale clustering of IRAS galaxies, *Mon. Not. R. Astron. Soc.*, **247**, 10P, 1990.

Fisher, K. B., M. Davis, M. A. Strauss, A. Yahil, and J. Huchra, Clustering in the 1.2-Jy IRAS Galaxy Redshift Survey. I—The redshift and real space correlation functions, *Mon. Not. R. Astron. Soc.*, **266**, 50, 1994.

Fisher, K. B., J. P. Huchra, M. A. Strauss, M. Davis, A. Yahil, and D. Schlegel, The IRAS 1.2 Jy survey: Redshift data, *Astrophys. J. Suppl. Ser.*, **100**, 69, 1995.

Gilli, R., E. Daddi, R. Chary, M. Dickinson, D. Elbaz, M. Giavalisco, M. Kitzbichler, D. Stern, and E. Vanzella, The spatial clustering of mid-IR selected star forming galaxies at z ˜ 1 in the GOODS fields, *Astron. Astrophys.*, **475**, 83–99, 2007.

Gonzalez-Solares, E. A., S. Oliver, C. Gruppioni, F. Pozzi, C. Lari, M. Rowan-Robinson, S. Serjeant, F. La Franca, and M. Vaccari, Large-scale structure in the ELAIS S1 Survey, *Mon. Not. R. Astron. Soc.*, **352**, 44–48, 2004.

Hamilton, A. J. S., Omega from the anisotropy of the redshift correlation function in the IRAS 2 Jansky survey, *Astrophys. J.*, **406**, L47–L50, 1993.

Iyengar, K. V. K., T. N. Rengarajan, and R. P. Verma, Properties of IRAS galaxies with $B(0)_T$ not greater than approximately 14.5, *Astron. Astrophys.*, **148**, 43–51, 1985.

Kawada, M. *et al.*, The Far-Infrared Surveyor (FIS) for AKARI, *Publ. Astron. Soc. Jpn.*, **59**, 389–400, 2007.

Lagache, G. and J. L. Puget, Detection of the extra-Galactic background fluctuations at 170 μm, *Astron. Astrophys.*, **355**, 17–22, 2000.

Lahav, O., R. J. Nemiroff, and T. Piran, Relative bias parameters from angular correlations of optical and IRAS galaxies, *Astrophys. J.*, **350**, 119–124, 1990.

Landy, S. D. and A. S. Szalay, Bias and variance of angular correlation functions, *Astrophys. J.*, **412**, 64–71, 1993.

Liu, B., G. Wang, X. Y. Xia, and Z. G. Deng, Two-dimensional analysis of galaxies from IRAS faint sources catalog, *Acta Astrophys. Sinica*, **14**, 207, 1994.

Maddox, S. J. *et al.*, Herschel-ATLAS: The angular correlation function of submillimetre galaxies at high and low redshift, *Astron. Astrophys.*, **518**, L11, 2010.

Magliocchetti, M., M. Cirasuolo, R. J. McLure, J. S. Dunlop, O. Almaini, S. Foucaud, G. de Zotti, C. Simpson, and K. Sekiguchi, On the evolution of clustering of 24-μm-selected galaxies, *Mon. Not. R. Astron. Soc.*, **383**, 1131–1142, 2008.

Magliocchetti, M. *et al.*, The PEP survey: clustering of infrared-selected galaxies and structure formation at $z \sim 2$ in GOODS-South, *Mon. Not. R. Astron. Soc.*, **416**, 1105–1117, 2011.

Małek, K., A. Pollo, T. T. Takeuchi, P. Bienias, M. Shirahata, S. Matsuura, and M. Kawada, Star forming galaxies in the AKARI deep field south: identifications and spectral energy distributions, *Astron. Astrophys.*, **514**, A11, 2010.

Matsuhara, H. *et al.*, ISO deep far-infrared survey in the "Lockman Hole". II. Power spectrum analysis: evidence of a strong evolution in number counts, *Astron. Astrophys.*, **361**, 407–414, 2000.

Matsuura, S., M. Shirahata, M. Kawada, T. T. Takeuchi, D. Burgarella, D. L. Clements, W.-S. Jeong, H. Hanami, S. A. Khan, H. Matsuhara, T. Nakagawa, S. Oyabu, C. P. Pearson, A. Pollo, S. Serjeant, T. Takagi, and G. J. White, Detection of the cosmic far-infrared background in AKARI deep field south, *Astrophys. J.*, **737**, 2, 2011.

Meiksin, A. and M. Davis, Anisotropy of the galaxies detected by IRAS, *Astron. J.*, **91**, 191–198, 1986.

Mo, H. J., Y. P. Jing, and G. Boerner, On the error estimates of correlation functions, *Astrophys. J.*, **392**, 452–457, 1992.

Murakami, H. *et al.*, The infrared astronomical mission AKARI, *Publ. Astron. Soc. Jpn.*, **59**, S369–376, 2007.

Murphy, E. J. *et al.*, Calibrating extinction-free star formation rate diagnostics with 33 GHz free-free emission in NGC 6946, *Astrophys. J.*, **737**, 67, 2011.

Neugebauer, G. *et al.*, The Infrared Astronomical Satellite (IRAS) mission, *Astrophys. J.*, **278**, L1–L6, 1984.

Norberg, P., C. M. Baugh, E. Gaztañaga, and D. J. Croton, Statistical analysis of galaxy surveys—I. Robust error estimation for two-point clustering statistics, *Mon. Not. R. Astron. Soc.*, **396**, 19–38, 2009.

Oliver, S. *et al.*, Angular clustering of galaxies at 3.6 microns from the Spitzer Wide-area Infrared Extragalactic (SWIRE) survey, *Astrophys. J. Suppl. Ser.*, **154**, 30–34, 2004.

Onaka, T. *et al.*, The Infrared Camera (IRC) for AKARI—Design and imaging performance, *Publ. Astron. Soc. Jpn.*, **59**, 401, 2007.

Peacock, J. A., The evolution of galaxy clustering, *Mon. Not. R. Astron. Soc.*, **284**, 885–898, 1997.

Peacock, J. A. and S. J. Dodds, Reconstructing the linear power spectrum of cosmological mass fluctuations, *Mon. Not. R. Astron. Soc.*, **267**, 1020, 1994.

Peebles, P. J. E., *The Large Scale Structure of the Universe*, Princeton University Press, Princeton, 1980.

Planck Collaboration, Planck early results. XVIII. The power spectrum of cosmic infrared background anisotropies, *Astron. Astrophys.*, **536**(A18), 2011.

Pollo, A., P. Rybka, and T. T. Takeuchi, Star-galaxy separation by far-infrared color-color diagrams for the AKARI FIS all-sky survey (bright source catalog version β-1), *Astron. Astrophys.*, **514**, A3, 2010.

Rowan-Robinson, M. and G. Needham, The two-dimensional covariance function for IRAS sources, *Mon. Not. R. Astron. Soc.*, **222**, 611–617, 1986.

Rowan-Robinson, M., W. Saunders, A. Lawrence, and K. Leech, The QMW IRAS galaxy catalogue—A highly complete and reliable IRAS 60-micron galaxy catalogue, *Mon. Not. R. Astron. Soc.*, **253**, 485–495, 1991.

Rybka, P., A. Pollo, and T. T. Takeuchi, Classification schemes and properties of infrared galaxies, *Publ. Korean Astron. Soc.*, **27**, 293–294, 2012.

Rybka, P., A. Pollo, and T. T. Takeuchi, 2013 (in preparation).

Saunders, W., M. Rowan-Robinson, and A. Lawrence, The spatial correlation function of IRAS galaxies on small and intermediate scales, *Mon. Not. R. Astron. Soc.*, **258**, 134–146, 1992.

Saunders, W. *et al.*, The PSCz catalogue, *Mon. Not. R. Astron. Soc.*, **317**, 55–63, 2000.

Schlegel, D. J., D. P. Finkbeiner, and M. Davis, Maps of dust infrared emission for use in estimation of reddening and cosmic microwave background radiation foregrounds, *Astron. Astrophys.*, **500**, 525–553, 1998.

Strauss, M. A., J. P. Huchra, M. Davis, A. Yahil, K. B. Fisher, and J. Tonry, A redshift survey of IRAS galaxies. VII—The infrared and redshift data for the 1.936 Jansky sample, *Astrophys. J. Suppl. Ser.*, **83**, 29–63, 1992.

Takeuchi, T. T., V. Buat, S. Heinis, E. Giovannoli, F.-T. Yuan, J. Iglesias-Páramo, K. L. Murata, and D. Burgarella, Star formation and dust extinction properties of local galaxies from the AKARI-GALEX all-sky surveys. First results from the most secure multiband sample from the far-ultraviolet to the far-infrared, *Astron. Astrophys.*, **514**, A4, 2010.

Tomita, A., Y. Tomita, and M. Saitō, A variation in the present star formation activity of spiral galaxies, *Publ. Astron. Soc. Jpn.*, **48**, 285–303, 1996.

White, S. D. M. and M. J. Rees, Core condensation in heavy halos—A two-stage theory for galaxy formation and clustering, *Mon. Not. R. Astron. Soc.*, **183**, 341–358, 1978.

Yamamura, I., S. Makiuti, N. Ikeda, Y. Fukuda, S. Oyabu, T. Koga, and G. J. White, *AKARI/FIS All-Sky Survey Bright Source Catalogue Version 1.0 Release Note*, ISAS/JAXA, 2010.

A. Pollo (e-mail: apollo@fuw.edu.pl), T. T. Takeuchi, T. L. Suzuki, and S. Oyabu